Original Research Article

Synthesis, Spectral and Thermal Characterization of Selected Metal Complexes Containing Schiff Base Ligands with Antimicrobial Activities

Abstract

Selected metal complexes of Ni(II), Zn(II), Mn(II), Sn(II), Co(II) and Cd(II) ions were synthesized with three different synthesized Schiff base ligands. The ligands and metal complexes were isolated in the solid state from the reaction medium and characterized by molar conductivity measurement, magnetic susceptibility, Infrared, electronic spectral, thermal analysis and some physical measurements. The overall reactions were monitored by TLC analysis. Molar conductance study has shown that all the complexes were non-electrolytic in nature. FTIR studies suggested that Schiff bases act as deprotonated bidentate ligands and metal ions are attached with the ligands through N, O/S coordinating sites during complexation reaction. Magnetic susceptibility data coupled with electronic spectra revealed that Zn(II), Mn(II), Sn(II), and Cd(II) complexes have tetrahedral, Ni(II) complexes have a square planer and Co(II) complexes have octahedral geometry. Thermal analysis (TGA and DTG) data showed the possible degradation pathway of the complexes and also indicated that most of the complexes were thermally stable up to 200^0C. The Schiff bases and their metal complexes have been found moderate to strong antimicrobial activity.

Keywords: Schiff Base, Thiosemicarbazide, TGA, DTG, Antimicrobial activity

1. INTRODUCTION

Multidentate ligands are extensively used for the preparation of metal complexes with interesting properties [1-5]. Among these ligands, Schiff bases containing nitrogen and phenolic oxygen donor atoms are of considerable interest due to their potential application in catalysis, medicine and material science [6-9]. Transition metal complexes of these ligands exhibit varying configurations, structural liability and sensitivity to molecular environments. The central metal ions in these complexes act as active sites for pharmacological agent. This feature is employed for modelling active sites in biological systems.

Thiosemicarbazones obtained by the condensation reaction of thiosemicarbazide and different aldehydes or ketones are important chemicals due to their broad profile of pharmacological activity. The transition metal complexes of thiosemicarbazone are also played important role in antimicrobial, antitumour and anticancer activities.

Therefore, in view of our interest in the synthesis of new Schiff base complexes, which might find application as pharmacological and as luminescence probes, we have synthesized and characterized new transition metal complexes of Schiff bases formed by the condensation reaction of different aldehydes and amino acids. The results of our studies are presented in this article.

2. Experimental

2.1 Materials and Methods

All chemicals and solvents used were of the Analar grade. All metal(II) salts were used as chloride and sulphate. The solvents such as Ethanol, methanol, chloroform, Diethyl ether, petroleum ether, DMSO (dimethyl sulfoxide) and acetonitrile were purified by standard procedure. The melting point or the decomposition temperature of all the prepared ligand and metal complexes were observed in an electrothermal melting point apparatus model No. AZ6512. Vibrational spectra (IR) were recorded with a NICOLET 310, FTIR spectrophotometer, Belgium, in the range 4000-225 cm^{-1} with a KBr disc as a reference. UV-Visible spectra of the complexes in DMSO ($0.5x\ 10^{-3}$M) were recorded in the region 200-800 nm on a Thermoelectron Nicolet evolution 300 UV-Visible spectrophotometer. The SHERWOOD SCIENTIFIC Magnetic Susceptibility Balance that following the Gouy Method were used to measure the magnetic moment of the solid complexes. The electrical conductance measurements were made at room temperature in freshly prepared aqueous solution (10^{-3} M) and in DMSO using a WPACM35 conductivity meter and a dip-cell with a platinum electrode. The thermogravimetric analyses (TGA) were performed on Perkin Elmer Simultaneous Thermal Analyzer, STA-8000. The purity of the ligand and metal complexes were tested by Thin Layer Chromatography (TLC).

2.1 Synthesis of Schiff base Ligand $C_8H_9ON_3S$ (L^1)

The ligand was prepared by condensation reaction of 20 mmoles of salisylaldehyde (1.048ml) with 20 mmole (1.82gm) of thiosemicarbazide in a clean round-bottomed flask. Salisylaldehyde was dissolved in 20ml ethanol and thiosemicarbazide was dissolved in hot ethanol with water. The solutions were mixed and refluxed for 3-4 hours. On cooling off-white colored product was formed which was washed with ethanol, acetone, and diethyl ether and dried in vacuum desiccators over anhydrous $CaCl_2$. The purity of ligand was tested by TLC using different solvents. The product was found to be soluble in methanol, chloroform and DMSO. It provided 80% yield at 34°C. The target Schiff base was synthesized according to Schema-1.

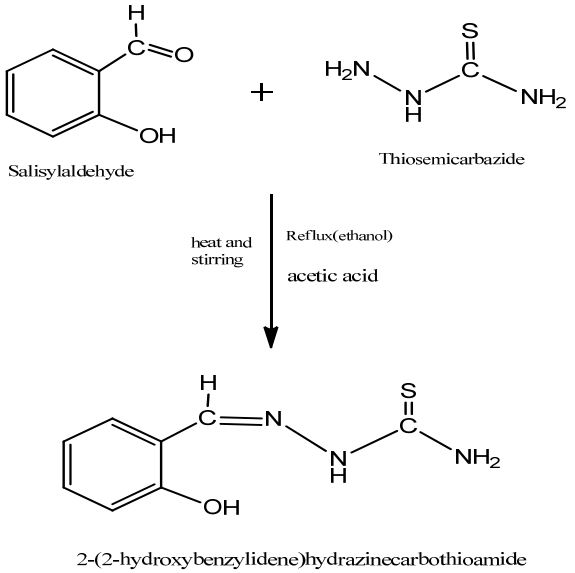

Schema 1: Synthetic pathway of Schiff base ligand $C_{14}H_{11}O_3N$ (L^1)

2.3 Synthesis of Metal Complexes Using Schiff Base Ligand $C_{14}H_{11}O_3N$ (L^1)

The synthesized complexes have the general formula $[M(SB)_2]$; where M= Zn(II), Ni(II) and Mn(II) and SB = synthesized Schiff base ligand (Schema 2). During complexation reaction,15ml methanolic solution of Zinc(II) sulphate (0.2875g, 1mmol)/ Ni(II) chloride hexahydrate (0.238g, 1mmol)/ Manganese(II) chloride tetrahydrate (0.198g, 1mmol) was taken in a two-necked round bottom flask and kept on a magnetic stirring. A methanolic solution (20 mL) of prepared Schiff base ligand (0.390g, 2mmol) was added dropwise and a methanolic solution (10mL) of KOH (0.1122g,1mmol) was added slowly then the resultant mixture was heated with constant stirring on a magnetic stirrer for 4-5 hours. On cooling colored solid product was formed which was washed with methanol, acetone, ether and dried in vacuum over anhydrous $CaCl_2$. The reaction was monitored by TLC using petroleum ether, toluene, ethyl acetate and methanol as solvent. The common structure of metal complexes has been shown in Schema-1 and individual expected structures of the complexes are shown as supplementary materials.

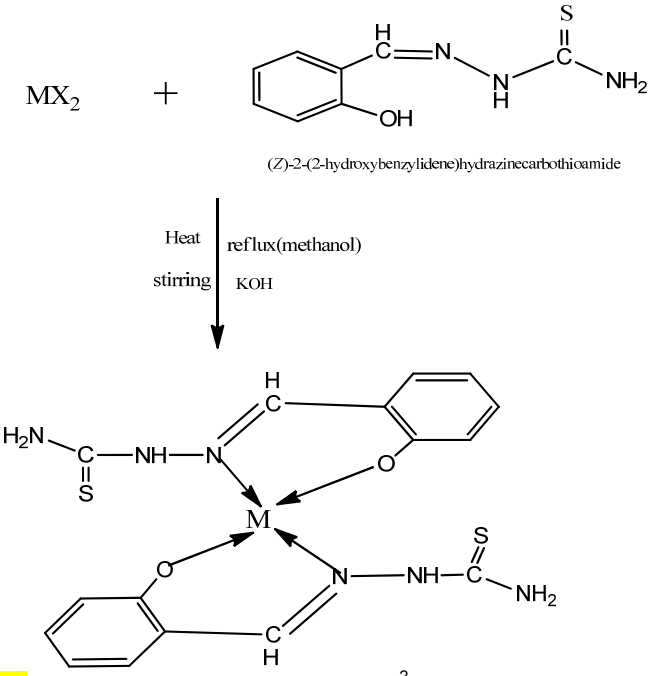

Schema 2: Synthetic pathway of Schiff Base Ligand (L^2) Metal Complexes, with M=Zn(II), Ni(II), Mn(II), and Sn(II) ions and X=Cl^-,SO_4^{2-} ions

2.4 Synthesis of Schiff Base Ligand $C_{14}H_{11}O_3N$ (L^2)

4-hydroxy benzaldehyde (2.44g, 20 mmol) dissolved in absolute ethanol (20-25 mL) was added dropwise to a constant stirring solution of 4-aminobenzoic acid(2.76 g, 20 mmol) in 30 mL ethanol and 2 mL of conc. glacial acetic acid was added slowly. Then the mixture was refluxed for (4-5)h. On cooling, a solid yellow product was formed which was filtered, washed with ethanol and diethyl ether and dried in vacuum over anhydrous $CaCl_2$. The reaction was monitored by TLC using petroleum ether, ethyl acetate, toluene and methanol solvents. The product was found to be soluble in methanol, chloroform and DMSO. It provided 65% yield at 34°C. The target Schiff base was synthesized according to Schema-3.

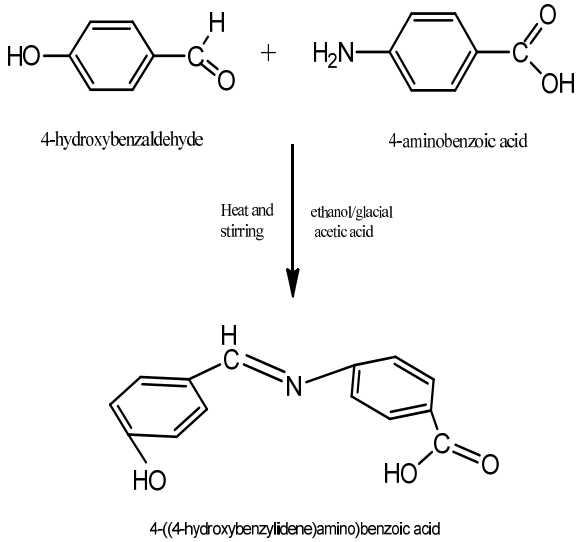

Schema-3: Synthetic pathway of Schiff base ligand $C_{14}H_{11}O_3N$ (L^2)

2.5 Synthesis of Metal Complex Using Schiff Base Ligand (L^2)

The complex was prepared in 1:2 molar ratio (metal: ligand). A methanolic solution (20 mL) of cobalt(II) chloride hexahydrate (0.24 g, 1 mmol)) was taken in a two-necked round bottom flask and kept on magnetic stirring and a methanolic solution (20 mL) of prepared Schiff base ligand (0.483 g, 2

mol) was added dropwise and stirred with heating for 4-5h. On cooling, the precipitate was formed which was filtered, washed with ethanol, acetone, and diethyl ether and dried in vacuum desiccators over anhydrous $CaCl_2$. The purity of complex was tested by TLC using different solvents. The complex was soluble in DMSO with heat. The proposed structure of the complex is shown in Schema-4.

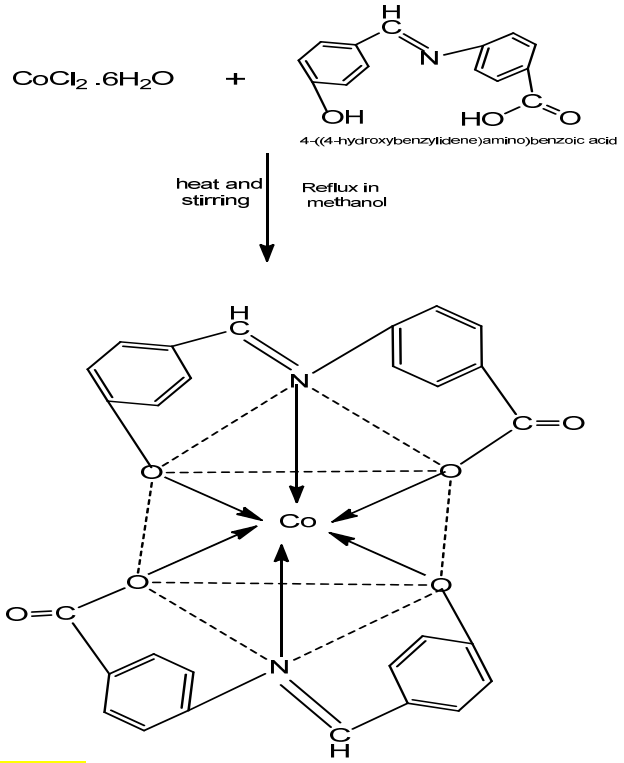

Schema-4: Synthetic pathway of Co(II) complex with Schiff Base Ligand (L^2)

2.6 Synthesis of Schiff base Ligand $C_9H_{11}N_3OS$ (L^3)

To a stirring solution of thiosemicarbazide (0.91 gm, 10 mmol) dissolved in 20mL of ethanol with water, a solution of Anisaldehyde(1.22mL,10mmol) in 10mL ethanol was added dropwise. After sometime 2ml of glacial acetic acid was added with the reaction mixture and the solution was refluxed for 5-6 h and allowed to cool overnight in room temperature. The off-white product was filtered washed several times with ethanol and finally with diethyl ether and dried in vacuum over anhydrous $CaCl_2$. The reaction was monitored by TLC using petroleum ether, ethyl acetate, toluene and methanol solvents.The product was found to be soluble in methanol, DMF and DMSO. It provided 62% yield. The Schiff base was synthesized according to Schema-5.

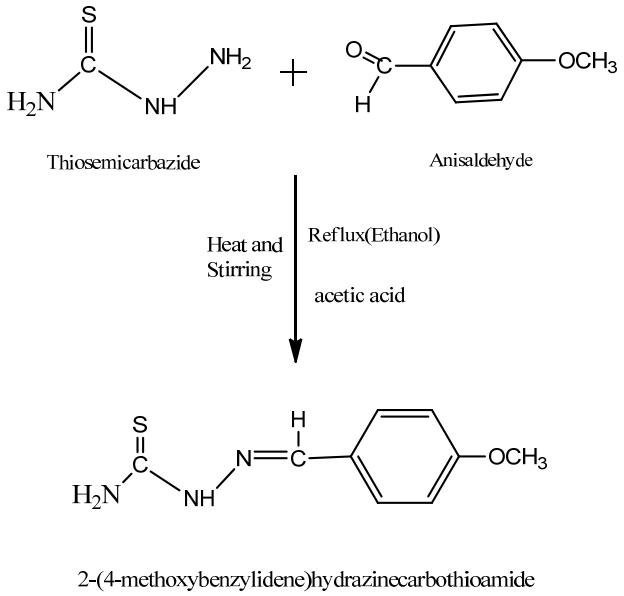

Schema-5: Synthetic pathway of Schiff base ligand $C_9H_{11}N_3OS$ (L^3)

2.7 Synthesis of Metal Complex Using Schiff Base Ligand (L^3):

The complex was prepared in 1:2 molar ratio (metal: ligand). Methanolic solution (20 mL) of cadmium(II) chloride dihydrate (0.228g, 1mmol) was taken in a two-necked round bottom flask and kept on magnetic stirring. A methanolic solution (20 mL) of prepared Schiff base ligand (L^3) (0.418g, 2mmol) was added dropwise and stirred with heating for 4-5h. On cooling, the precipitate was formed which was filtered, washed with ethanol, acetone, and diethyl ether and dried in vacuum desiccators over anhydrous $CaCl_2$. The reaction was monitored by TLC using different solvents. The complex was soluble in DMSO with heat. The proposed structure of the complex is shown in Scheme-6.

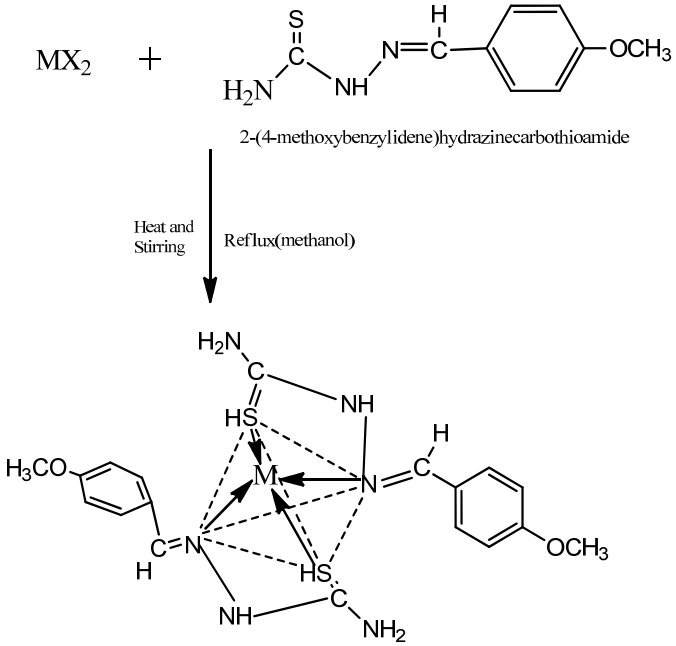

Schema-6: Synthetic pathway of Schiff Base Ligand (L^4) Metal Complex
Where, M=Cd(II) ions

3. Characterization of the Ligands and Complexes

The structures of the complexes were characterized by melting point, conductivity measurements, magnetic susceptibility, IR spectra and UV visible spectra [10] analysis. The purity of the ligands and

metal complexes were monitored by Thin Layer Chromatography (TLC). The ligands and complexes are characterized below by these methods.

3.1 Melting point

Melting point gives an approximate idea about the nature of the complexes and can suggest whether it is covalent or ionic [11]. The melting point of all the synthesized ligands and complexes are shown in Table-1.

Table-1: Physical characteristics and analytical data of ligands and complexes

Compound/Empirical Formula	Formula Weight	Color	Yield(%)	Melting Point/ Decomposition temp.(^{0}C)
Ligand (L^1) $C_8H_9ON_3S$	195	off white	80 %	215^{0}C - 217^{0}C
[Zn (L^1)$_2$] .2H_2O [$ZnC_{16}H_{16}O_2N_6S_2$].2H_2O	491.38	cream color	67 %	above 300^{0}C
[Ni (L^1)$_2$].H_2O [$NiC_{16}H_{16}O_2N_6S_2$].H_2O	466.93	yellow green	70 %	275^{0}C - 280^{0}C
[Mn (L^1)$_2$] .H_2O [$MnC_{16}H_{16}O_2N_6S_2$].H_2O	462.94	golden rod	65 %	275^{0}C - 280^{0}C
[Sn (L^1)$_2$] [$SnC_{16}H_{16}O_2N_6S_2$]	508.71	greenish yellow	60%	240^{0}C - 250^{0}C
Ligand (L^2) $C_{14}H_{11}O_3N$	241	yellow	65 %	241^{0}C - 245^{0}C
[Co(L^2)$_2$] .2H_2O [$CoC_{28}H_{18}O_6N_2$].2H_2O	576.93	golden rod	56 %	above 300^{0}C
Ligand (L^3) $C_9H_{11}N_3OS$	209	off white	62%	145^{0}C - 150^{0}C
[Cd(L^3)$_2$] [$CdC_{18}H_{22}O_2N_6S_2$]	530.41	white	75 %	260^{0}C - 265^{0}C

3.2 Conductivity

The molar conductivities were obtained using the formula

$$\Lambda = \frac{1000}{C} \times \text{Cell constant} \times \text{Observed conductivity}, \quad (1).$$

where, Λ=molar conductance, C= concentration.
The molar conductance is calculated from the measured specific conductance at room temperature by using the above equation. The experimental results are shown in Table-2.

Table-2: Data for the determination of Molar conductivity

Name of Complex	Observed conductivity (ohm^{-1} cm^2 mol^{-1})	Molar conductance $\Lambda = (1000/c) \times specificconductance$ Scm^2mol^{-1}	μ_{eff} in B.M.	No. of unpaired electron
$[Zn(L^1)_2].2H_2O$ $[ZnC_{16}H_{16}O_2N_6S_2].2H_2O$	3	3	0.567	–
$[Ni(L^1)_2].H_2O$ $[NiC_{16}H_{16}O_2N_6S_2].H_2O$	6	6	1.471	–
$[Mn(L^1)_2].H_2O$ $[MnC_{16}H_{16}O_2N_6S_2].H_2O$	8	8	2.576	1
$[Sn(L^1)_2]$ $[SnC_{16}H_{16}O_2N_6S_2]$	9	9	0.639	–
$[Co(L^2)_2].2H_2O$ $[CoC_{28}H_{18}O_6N_2].2H_2O$	8	8	4.017	3
$[Cd(L^3)_2]$ $[CdC_{18}H_{22}O_2N_6S_2]$	6	6	0.461	–

From the above table data, it is showed that all the complexes are non-electrolyte.

3.3 Characterizations by Magnetic Susceptibility

Measurement of magnetic susceptibility: The measurements of magnetic susceptibilities were made at about constant temperature; Curie-law was used and was calculated from the equation.

$$\mu_{eff} = 2.83 \sqrt{\chi_m^{corr}} .T \quad B.M. \qquad (2)$$

Thus μ_{eff} obtained is known as the effective magnetic moment. All the values and weight were expressed in C.G.S. units. The observed values of the effective magnetic moment (μ_{eff}) of the complexes at room temperature are given in table 2. From the above data, it is showed that the Zn(II), Ni(II), Sn(II) and Cd(II) ions complexes are diamagnetic and Mn(II) and Co(II) ions complexes are paramagnetic in nature[13].

3.4 Measurement of IR spectra: At first the complexes heat six hours and KBr overnight in the oven. Then the complexes and KBr grind with a pestle in a mortar. Infrared spectra disc were recorded as KBr with a NICOLET 310, FTIR spectrophotometer, Belgium, from 4000-225 cm^{-1}.

3.4.1 IR spectra of Schiff Base ligand $C_8H_9ON_3S$ (L^1) and It's metal complexes

The spectrum of ligand showed a strong absorption band at 1616 cm^{-1} due to the azomethine υ(C=N) stretching frequency of the free ligand [14-18] indicating that the condensation has taken place between the CHO moiety of salisylaldehyde and $–NH_2$ moiety of thiosemicarbazide. The IR spectra of the free ligand (figure-1) showed two bands at 3320 cm^{-1} and 3174 cm^{-1} may be attributed to the free -NH_2 and υ(N–H) groups respectively. These bands remain in the same region in all complexes spectra, suggesting nonparticipation in the coordination of one terminal $–NH_2$ group in thiosemicarbazone [15,19-21] The band observed at 3444 $cm^{-1}$was assigned to the υ(O-H) of hydroxyl group [14,15,22]. The strong band 776 cm^{-1} for υ(C=S) indicated that C=S bond was present in the Schiff base ligand [14,22].

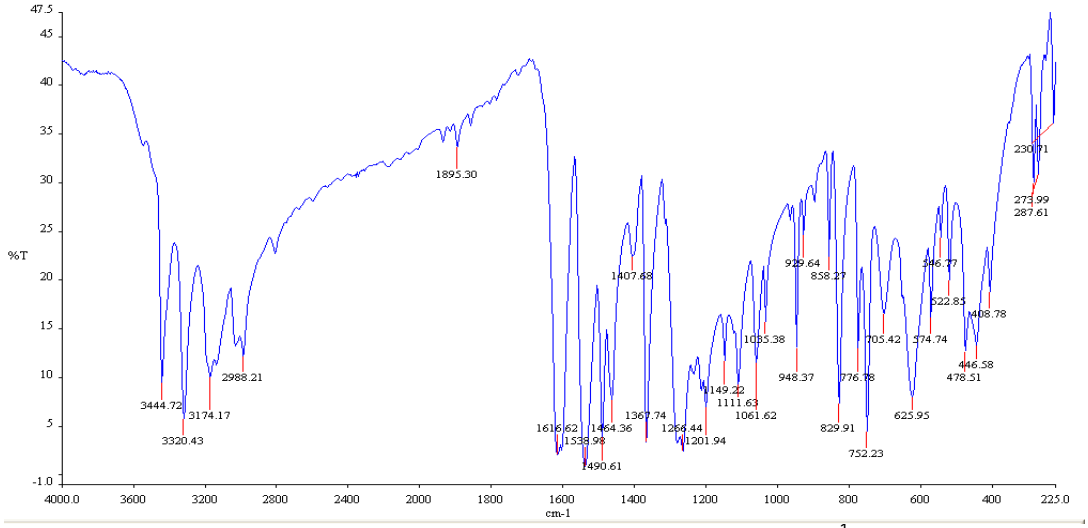

Figure-1: IR spectra of Schiff base ligand $C_8H_9ON_3S$ (L^1)

In order to determine the mode of coordination of ligand to metal in complexes, IR spectrum of the ligand was compared with IR spectrum of metal complexes (figure-2). The band at 1616 cm^{-1} due to the azomethine υ(C=N) stretching frequency of the free ligand that shifted to a lower frequency in the spectra of the Zn (II) complex at 1607 cm^{-1} which indicated the coordination through azomethine N atom. The band 3444 cm^{-1} due to the υ(O-H) of the hydroxyl group in the IR spectra of the ligand was absent and shifted to lower absorption frequency in the IR spectra of Ni(II) complex indicated the coordination through the phenolic oxygen [23,24]. This is confirmed by the shift of υ(C-O) stretching vibration observed at 1266cm^{-1} in the spectra of free ligand to 1285 cm^{-1} stretching vibration of complex after coordination [16], which corresponds to forming of weaker C-O(Zn) bond comparing to C-O(H) and confirms coordination of ligand to Ni(II) via deprotonated phenolic oxygen [25,26]. Also the medium intensity bands observed at 566 $cm^{-1}$is attributed to M-O and 448 cm^{-1} is attributed to M-N bonds [27]. IR spectral components of the synthesized complexes are shown in Table – 3.

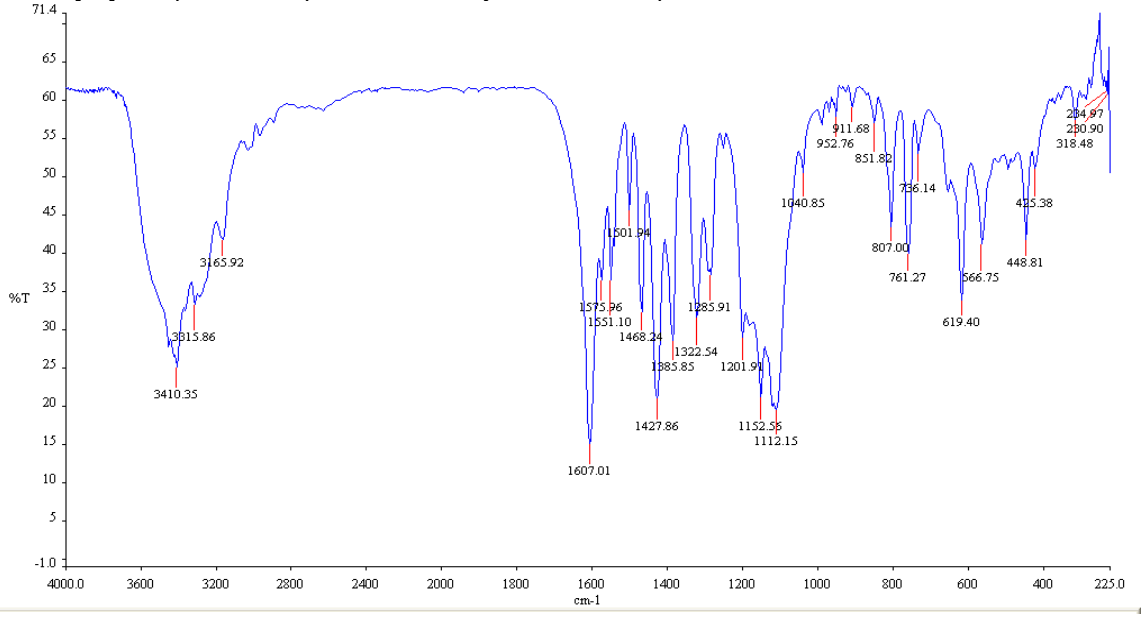

Figure-2: IR spectra of $[ZnC_{16}H_{16}O_2N_6S_2].2H_2O$ complex

Table-3: FTIR spectral data of the ligand $C_8H_9ON_3S$ (L^1) and it's metal complexes (in cm^{-1})

Ligand / Metal Complexes	IR/cm^{-1}				
	ν(O-H)	ν(C=N)	ν(C-O)	ν(M-O)	ν(M-N)

$C_8H_9ON_3S$	3444	1616	1266	-	-
$[ZnC_{16}H_{16}O_2N_6S_2].2H_2O$	3410	1607	1285	566	448
$[NiC_{16}H_{16}O_2N_6S_2].H_2O$	3412	1607	1294	567	457
$[MnC_{16}H_{16}O_2N_6S_2].H_2O$	3413	1600	1296	570	442
$[SnC_{16}H_{16}O_2N_6S_2]$	3436	1610	1286	594	458

3.4.2 IR spectra of Schiff Base ligand $C_{14}H_{11}O_3N$ (L^2) and It's metal complex

The bands at 1735 cm^{-1} and 3420 cm^{-1} due to carbonyl (C=O) and NH_2 stretching vibrations of the starting reagents respectively were absent in the spectra of ligand and a strong new band at 1620 cm^{-1} appeared which assigned to the azomethine (HC=N) linkage, a fundamental feature of Schiff base ligand [28,29]. This indicated that amino and aldehyde moieties of the starting reagents have been converted into the azomethine moiety. The bands at 1320 cm^{-1} due to υ(C-O) of the phenolic group and 3410 cm^{-1} due to the phenolic υ(OH) were also observed in the spectra of ligand [23]. The bands at 1680 cm^{-1} due to υ(C=O) stretching vibration and 3080 cm^{-1} due to carboxylic – υ(OH) were observed in the IR spectra of ligand [30-33].

The band at 1620 cm^{-1} due to the azomethine –HC=N stretching vibration was shifted to a lower frequency at 1541 cm^{-1} in the metal complex compared to free ligand, suggested the coordination of metal ion through nitrogen of azomethine group [34-36]. The N atom of azomethine would reduce the electron density in the azomethine link and thus lower the –HC=N absorption after coordination. This is further substantiated by the presence of a new band at 457 cm^{-1} assignable to υ(M-N). The disappearance of phenolic υ(OH) band at 3410 cm^{-1} in Co(II) complex suggested the coordination by the phenolic oxygen after deprotonation to the metal ions. This is further supported by shifting of υ(C-O) phenolic band at 1320 cm^{-1} to lower wave number at 1305 cm^{-1} in the metal complex. The appearance of a new band at 590cm^{-1} due to υ(M-O) in the Co(II) complex which further substantiates. The band at 1680 cm^{-1} assigned to υ(C=O) in the spectra of ligand also shifted to the lower frequency range in the metal complex. That suggested the involvement of oxygen atom of carboxylic υ(-OH) group to the coordination with metal ions. The comparison of the IR spectra of the Schiff base and it's metal chelates indicated that the Schiff base ligand coordinated to metal ions by three donor atoms representing the ligand acting in a tri-dentative manner. Spectral data of $[CoC_{28}H_{18}O_6N_2].2H_2O$ is shown in Table 4.

In order to determine the mode of coordination of ligand to metal in complexes IR spectrum of the ligand was compared with IR spectrum of metal complexes [14, 23]. The band at 1616 cm^{-1} due to the azomethine υ(C=N) stretching frequency of the free ligand that shifted to a lower frequency in the spectra of the Ni(II) complex (figue-13) at 1607cm^{-1} indicating the coordination through N atom [5-9]. The band 3444 cm^{-1} due to the υ (O-H) of the hydroxyl group in the IR spectra of the ligand was absent and shifted to lower absorption frequency in the IR spectra of Ni(II) complex indicated the coordination through the phenolic oxygen [22,24]. This is confirmed by the shift of υ(C-O) stretching vibration observed at 1266 cm^{-1} in the spectra of free ligand to 1294 cm^{-1} stretching vibration of complex after coordination [16], which corresponds to forming of weaker C-O(Ni) bond comparing to C-O(H) and confirms coordination of ligand to Ni(II) via deprotonated phenolic oxygen. Also, the medium intensity bands observed at 567 $cm^{-1}$is attributed to M-O and 457cm^{-1} is attributed to M-N bonds [27].

The band at 1616 cm^{-1} due to the azomethine υ(C=N) stretching frequency of the free ligand that shifted to a lower frequency in the spectra of the Mn(II) complex at 1600 cm^{-1} indicating the coordination through N atom. The band 3444 cm^{-1} due to the υ(O-H) of the hydroxyl group in the IR spectra of the ligand was absent and shifted to lower absorption frequency in the IR spectra of Mn(II) complex indicated the coordination through the phenolic oxygen. This is confirmed by the shift of υ(C-

O) stretching vibration observed at 1266 cm^{-1} in the spectra of free ligand to 1296 cm^{-1} stretching vibration of complex after coordination , which corresponds to forming of weaker C-O(Mn) bond comparing to C-O(H) and confirms coordination of ligand to Mn(II) via deprotonated phenolic oxygen [5,17]. Also, the medium intensity bands observed at 570$cm^{-1}$is attributed to M-O and 442cm^{-1} is attributed to M-N bonds [27].

The band at 1616 cm^{-1} due to the azomethine υ(C=N) stretching frequency of the free ligand that shifted to a lower frequency in the spectra of the Sn(II) complex at 1610 cm^{-1} indicating the coordination through N atom. The band 3444 cm^{-1} due to the υ(O-H) of the hydroxyl group in the IR spectra of the ligand was absent and shifted to lower absorption frequency in the IR spectra of Sn(II) complex indicated the coordination through the phenolic oxygen. This is confirmed by the shift of υ(C-O) stretching vibration observed at 1266 cm^{-1} in the spectra of free ligand to 1286 cm^{-1} stretching vibration of complex after coordination, which corresponds to forming of weaker C-O(Sn) bond comparing to C-O(H) and confirms coordination of ligand to Sn(II) via deprotonated phenolic oxygen . Also, the medium intensity bands observed at 594$cm^{-1}$is attributed to M-O and 458cm^{-1} is attributed to M-N bonds.

Table-4: FTIR spectral data of the ligand L^2 and $[CoC_{28}H_{18}O_6N_2].2H_2O$ (in cm^{-1})

Ligand / Metal Complexes	IR/cm^{-1}					
	v(O-H)	v(C=N)	v(C=O)	v(C-O)	v(M-O)	v(M-N)
$C_{14}H_{11}O_3N$	3410	1620	1680	1320	-	-
$[CoC_{28}H_{18}O_6N_2].2H_2O$	3436	1541	1598	1305	590	457

3.4.3 IR spectra of Schiff Base ligand $C_9H_{11}N_3OS$ (L^3) and Its metal complex

The peaks obtained at 3406cm^{-1} and 3291cm^{-1}may be assigned to symmetric and asymmetric υ(–N-H) stretching frequency of primary amino group. The broad peak obtained between 3282 and 2829 cm^{-1} may be assigned to overlapping of peaks of hydrogen-bonded υ(N-H) and aromatic C-H stretching frequency. The bands obtained between 1183 cm^{-1} and 1252 cm^{-1} in ligand were due to υ(-OCH_3)groups (Table-5). The peaks observed at 1606 cm^{-1} and 834 cm^{-1} may be assigned to υ(C=N) and υ(C=S) [37-39].

The bands at 1606 cm^{-1} and 834 cm^{-1} assigned to υ(C=N) and υ(C=S) modes and these bands shifted towards lower frequency in the spectra of Cd(II) complex (Table-5), which indicated that coordination takes place through nitrogen of υ(C=N) group and sulphur of υ(C=S) group. At lower frequency, the complex exhibited new bands at 540 and 397 cm^{-1} which further supported the coordination site υ(M–N) and υ(M–S) vibrations.

Table-5: FTIR spectral data of the ligand L^3 and its Cd(II) metal complex (in cm^{-1})

Ligand / Metal Complexes	IR/cm^{-1}			
	v(C=N)	v(C=S)	v(M-N)	v(M-S)
Ligand (L^3) $C_9H_{11}N_3OS$	1606	834	-	-
$[Cd(L^3)_2]$ $[CdC_{18}H_{22}O_2N_6S_2]$	1574	821	528	397

3.5 Characterization by UV-visible Spectra

The electronic spectral data for the ligand and their metal complex recorded in DMSO are summarized in Table-6. There are two absorption bands, assigned to n–π* and π–π* transitions, in the electronic spectrum of the ligand. These transitions are also found in the spectra of the complexes, but they are shifted towards lower and higher frequencies, indicating the coordination of the ligand to the metallic ions [40]. The UV spectra of the ligand show three absorption bands at 260nm,310nm and 355nm. The first two bands are assigned to π–π* transitions of azomethine chromospheres and a benzene ring and the third is assigned to n–π* transition of a lone pair of electrons of an azomethine nitrogen and an antibonding π orbital. The absorption band n-π*at 355 nm due to an imine group in the ligand, whereas for the zinc complex, the same was observed at 390 nm with weak absorption intensity which indicates the coordination of zinc with imine group [41]. The zinc complex shows only the charge transfer transition which can be assigned to charge transfer from the ligand to the metal and vice versa, no d-d transitions are expected for d^{10} Zn(II) complex [42].

The UV–Vis absorption spectra of the ligand and complex were recorded after dissolving into DMSO solvent at room temperature. There are two absorption bands, assigned to n–π* and π–π* transitions, in the electronic spectrum of the ligand. These transitions are also found in the spectra of the complexes, but they are shifted towards lower and higher frequencies, confirming the coordination of the ligand to the metallic ions [43]. The electronic spectrum of ligand exhibits three intense absorption peaks at 260 nm, 310 nm and 350nm. The first and second peaks were attributed to benzene π–π*and imino π–π*transitions and the third peak in the spectra was assigned to n–π*transition [44]. The electronic spectra of the Ni(II) complex with an electronic configuration of d^8 shows three new absorption bands in the visible region and these three bands of the transitions $^1A_{1g}\rightarrow{}^1A_{2g}$ (355nm), $^1A_{1g}\rightarrow{}^1B_{1g}$ (380nm) and $^1A_{1g}\rightarrow{}^1E_g$ (420 nm) were observed in the spectra of a square-planar Ni(II) complex [45,46].

The UV–Vis absorption spectra of the ligand and complex were recorded after dissolving into DMSO solvent at room temperature. There are two absorption bands, assigned to n–π* and π–π* transitions, in the electronic spectrum of the ligand. These transitions are also found in the spectra of the complexes, but the ligand to the metallic ions [47]. The electronic spectrum of ligand exhibits three intense absorption peaks at 260 nm, 310 nm and 350nm. The first and second peaks were attributed to benzene π–π*and imino π–π*transitions and the third peak in the spectra was assigned to n–π*transition. Due to Forbidden transition, several bands were observed in the visible region of Mn(II) complex, and the band at 430 nm is attributed to (d-d) transition of type $^6A_1\rightarrow{}^4T_2$.
The electronic absorption spectra of ligand L^1 and its Sn (II) complex in DMSO solution were carried out in the range of 200-800 nm at room temperature. There is a shift of the bands to longer wavelength in spectra of the complex is a good evidence of complex formation. There were various bands in the ligand spectra assigned to inter ligand and charge transfer of n-π* transitions according to their energies and intensities. Ligand exhibits three intense absorption peaks at 260 nm, 310 nm and 350nm. The first and second peaks were attributed to benzene π–π*and imino π–π*transitions and the third band in the spectra was assigned to n–π*transition . The complex showed an intense band at 410nm due to the n–π* transition of azomethine chromosphere and the band at 340 nm may be assigned as charge transfer band. It has been reported that the metal is capable of forming dn-pπ* bonds with ligands containing nitrogen as the donor atom. The Sn atom has its 5d orbital completely vacant and hence Sn←N bonding can take place by the acceptance of the lone pair of electrons from the azomethine nitrogen of the ligand [48-50].

Table-6: Magnetic moments and electronic spectral data for ligand (L^1) and its metal complexes

Compound	λ_{max} n.m	Wave number cm^{-1}	μ_{eff} B.M	Assignment
$C_8H_9ON_3S$	260 310 350	38461 32258 38571	–	π→π* π→π* n→π*

$[NiC_{16}H_{16}O_2N_6S_2].H_2O$	355 380 420	28169 26315 23809	1.469	$^1A_{1g}\rightarrow{}^1A_{2g}$ $^1A_{1g}\rightarrow{}^1B_{1g}$ $^1A_{1g}\rightarrow{}^1E_g$
$[ZnC_{16}H_{16}O_2N_6S_2].2H_2O$	265 320 390	37735 31250 25641	0.5197	C.T (M→L) C.T (M→L) C.T (M→L)
$[MnC_{16}H_{16}O_2N_6S_2].H_2O$	325 380 430	30769 26315 23255	2.507	$^6A_1\rightarrow{}^4T_2$

The magnetic moment and electronic spectra are very effective in the evaluation of results obtained by other methods of structural investigation. Information regarding the geometry of the complex of Co(II) ions was obtained from electronic spectral studies and magnetic moments (Table-7). The electronic spectra of ligand and their metal complexes were recorded in DMSO. Electronic spectrum of ligand shows strong absorption band at 330nm region can be assigned to the n→π*transition of the azomethine group of ligand, which slightly shifted to a lower frequency in the spectra of the complex, indicating that the azomethine nitrogen atom is involved in coordination to the metal ion. The Co(II) complex was found the magnetic moment 4.0137 B.M which indicated the three unpaired electrons per Co(II) ion attaining an octahedral environment [60]. The electronic spectrum of Co(II) complex shows bands at 264nm and 274nm are assignable to metal-ligand charge transfer band and the band 400nm is assignable to $^4T_{1g}(F)\rightarrow {}^4T_{1g}(P)$ transition.

Table-7: The electronic spectral data and magnetic moments for ligand (L^2) and it's metal complex

Compound	λ_{max} n.m	Wave number cm^{-1}	μ_{eff} B.M	Assignment
$C_{14}H_{11}O_3N$	330	30303	-	n→π*
$[CoC_{28}H_{18}O_6N_2].2H_2O$	264 274 400	37878 36496 25000	4.0137	Charge transfer(C.T) C.T (M→L) $^4T_{1g}(F)\rightarrow {}^4T_{1g}(P)$

The electronic spectral data for the ligand and it's metal complex recorded in DMSO are summarized in Table-8. There are two absorption bands, assigned to n–π* and π–π* transitions, in the electronic spectrum of the ligand. These transitions are also found in the spectra of the complexes, but they are shifted towards lower and higher frequencies, indicating the coordination of the ligand to the metallic ions. The UV spectra of the ligand show three absorption bands at 280nm,330nm and 350nm. The first two bands are assigned to π–π* transitions of azomethine chromospheres and a benzene ring and the third is assigned to n–π* transition of a lone pair of electrons of an azomethine nitrogen and an anti-bonding π orbital. The absorption band n-π*at 350nm due to an imine group in the ligand, whereas for the Cd(II) complex, the same was observed at 400 nm with weak absorption intensity which indicate the coordination of cadmium with imine group. The cadmium complex show only the charge transfer transition which can be assigned to charge transfer from the ligand to the metal and vice versa, no d-d transition are expected for diamagnetic d^{10} Cd(II) complex. The shifting of ligand absorption in the UV region, in the spectra of the complex confirming the coordination of the ligand to metal like Cd (II) ions.

Table-8: Magnetic moments and electronic spectral data for ligand (L^3) and it's Cd(II) Complex

Compound	λ_{max} n.m	Wave number cm^{-1}	μ_{eff} B.M	Assignment

$C_9H_{11}N_3OS$	280 330 350	35714 30303 28571	–	π→π* π→π* n→π*
$[CdC_{18}H_{22}O_2N_6S_2]$	295 340 400	33898 29412 25000	0.4606	C.T (M→L) C.T (M→L) C.T (M→L)

3.6 Thermogravimetric Analysis

3.6.1. Zn(II), Ni(II), Mn(II) and Sn(II) complexes of ligand $C_8H_9ON_3S$ (L^1)

The thermal decomposition analysis of solid Zn(II), Ni(II), Mn(II) and Sn(II) metal complexes were carried out under nitrogen atmosphere and heating rate was suitably controlled at 30°C min^{-1} and the weight loss was measured from the ambient temperature up to 800°C. The data from TGA and DTG clearly indicated that the decomposition of the complexes proceeds in three or four steps. There were some minor steps and asymmetry of TGA/DTG curves also observed. The weight losses for each complex were calculated within the corresponding temperature ranges. The different thermodynamic parameters are listed in Table-9 and the decomposition curves are shown as supplementary materials.

The TGA and DTG curve of Zn(II) complex indicated that the complex was decomposed into four main steps. In the first step of decomposition, two molecules of water were lost at the temperature range of 85-110°C (calculated 7.36%, experimental 7.20%). In this temperature range, the loss of water molecules indicates that the water molecules are of lattice type [51,52].In the temperature range 130-335°C (calculated 24.00% and experimental 23.10%), the part of ligand-$2CSNH_2$ was decomposed at the second step. The other part of the ligand $2C_6H_4O$- were decomposed in the third step at 335-740°C (calculated 37.50%, experimental 32 .00%). At above 750°C temperature the complex was decomposed and removed as Zn/ZnO (calculated 31.14%, experimental 37.70%) polluted with few carbon atoms [53].

The TGA and DTG curve of Ni(II) complex confirmed that the complex was decomposed into four main steps. The 1^{St} step involves the removal of one molecule of hydrated water (calculated 3.87%, experimental4.00% weight) at temperature range 80-190°C [54,55].In the 2^{nd} step the part of the ligand $2C_6H_4O^-$ was decomposed at 280-350°C (calculated 39.59%, experimental 34.82% weight). At the 3^{rd} step the fragmentation of coordinated ligand $2C_2H_4N_3$ S was decomposed from the complex at the temperature range 360-750°C (calculated 43.90%, experimental 44.20% weight) and above 750°C temperature the complex was completely decomposed and removed as Ni/NiO (calculated 12.64%, experimental 16.98%).

In the case of Mn(II) complex, the TGA and DTG curve indicated that the complex was decomposed into four main steps. At 1^{St} step, one molecule of hydrated water was removed at 80-180°C(calculated 3.90%, experimental 4.00%) [54,55]. Then the dehydrated complex was gradually decomposed and the part of ligand $2C_6H_4O^-$ was removed at the temperature range 180-350°C (calculated 39.92%, experimental 38.10%). The 3^{rd} step involves the decomposition of the ligand part $2CH_3N_2S$ at the temperature range 350-770°C(calculated 32.54%, experimental 32.22%). At above 770°C temperature finally the complex was completely decomposed and removed as Mn/MnO (calculated 23.64%, experimental 25.68%).

The Sn(II) complex showed high thermal stability and decomposed above 170 °C, indicating the absence of any lattice water molecules [69]. This complex was decomposed into four main steps. At first step, the part of ligand (-$2CH_2NS$) was decomposed at temperature 170-275°C (calculated 23.67%, experimental 22.00%). In 2^{nd} step, the decomposition of (-2CHN-) moiety was taken place at temperature 275-330°C (calculated 12.0%, experimental 10.65 %). The ligand part ($2C_6H_4O^-$) were decomposed at the 3^{rd} step at temperature range 330-750°C (calculated 36.29%, experimental 36.10 %) and finally, the complex was completely decomposed and removed as Sn/SnO (calculated 28.04%, experimental 31.25%).

Table- 9: Thermal data of Zn(II), Ni(II), Mn(II), Sn(II), Cd(II) and Co(II) complexes.

Complexes	Steps	Temperature Range/ °C	DTG Peak/ ^{0}C	TG mass loss% calc./found	Assignments
$[ZnC_{16}H_{16}O_2N_6S_2].2H_2O$	1st 2nd 3rd 4th	85-110 130-335 335-740 >750	97 278 350	7.36/7.20 24.00/23.10 37.50/32.00 31.14/37.7	$2H_2O$ $2CSNH_2$ $2C_6H_4O$- Zn/ZnO
$[NiC_{16}H_{16}O_2N_6S_2].H_2O$	1st 2nd 3rd 4th	80-190 280-350 360-750 >750	180 295 382	3.87/4.00 39.59/34.82 43.90/44.20 12.64/16.98	H_2O $2C_6H_4O^-$ $2C_2H_4N_3S$ Ni/NiO
$[MnC_{16}H_{16}O_2N_6S_2].H_2O$	1st 2nd 3rd 4th	80-180 180-350 350-770 >770	118 290	3.90/4.00 39.92/38.10 32.54/32.22 23.64/25.68	H_2O $2C_6H_4O^-$ $2CH_3N_2S$ Mn/MnO
$[SnC_{16}H_{16}O_2N_6S_2]$	1st 2nd 3rd 4th	170-275 275-330 330-750 >750	240 290 370	23.67/22.00 12.00/10.65 36.29/36.10 28.04/31.25	$2CH_2NS$ 2CHN- $2C_6H_4O^-$ Sn/SnO
$[CoC_{28}H_{18}O_6N_2].2H_2O$	1st 2nd 3rd 4th	40-110 110-480 480-650 >650	65 400 548	6.28/6.32 51.31/49.20 32.12/28.80 10.29/15.72	$2H_2O$ $2C_8H_5O_2N$ $2C_6H_4O^-$ Co/CoO
$[CdC_{18}H_{22}O_2N_6S_2]$	1st 2nd 3rd	230-455 455-740 >740	282 570	50.53/49.23 28.28/27.05 21.19/24.00	$2C_8H_8ON$ $2CH_3N_2S$ Cd/CdO

3.6.2. Co(II) complex of ligand $C_{14}H_{11}O_3N$ (L^2)

TGA was carried out for solid Co(II) metal complex under N_2 flow. The heating rate was suitably controlled at 30°C min^{-1} and the weight loss was measured from the ambient temperature up to 800°C. The thermogram of complex exhibits three clear-cut decomposition stages in (figure-3). The first stage with estimated mass loss of 6.32% (calculated mass loss 6.28%) within the temperature range 40–110°C corresponding to the loss of water molecules [56,57]. The second stage occurs at 110–480°C, with a mass loss of 49.20% (calculated 51.31%), corresponding to the loss of $2C_8H_5O_2N$ parts of the ligand. The third stage of decomposition occurs at the temperature range 480–650°C, with a mass loss of 28.80% (calculated 32.12%), corresponding to the loss of $2C_6H_4O$ moiety. At above 650°C temperature, the complex was completely decomposed and removed as of 15.72% (calculated 10.29%). The different TG and DTG data are given in Table-9.

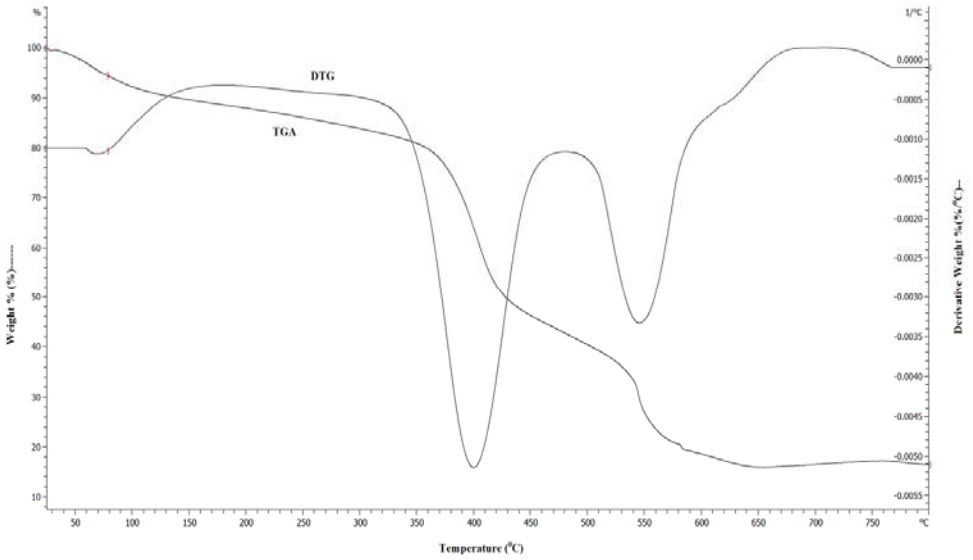

Figure-3: TGA and DTG curve of $[CoC_{28}H_{18}O_6N_2].2H_2O$

3.6.3. Cd(II) complex of ligand $C_9H_{11}N_3OS$ (L^3)

Thermogravimetric analysis of solid Cd(II) metal complex under N_2 flow. The heating rate was suitably controlled at 30°C min^{-1} and the weight loss was measured from the ambient temperature up to 800°C. The TGA curve of the Cd(II) complex showed no mass loss up to 230 °C, indicating the absence of lattice / coordinated water [58,59] and the high thermal stability of the complex. The thermogram of Cd(II) complex is given in Fig.4.24, which shows two stage decomposition pattern. The first stage was exhibited a maximum mass loss of 49.23% (calculated 50.53%) of ligand part ($2C_8H_8ON$) at 230-455°C. The second stage occurs at 455–740°C, with a mass loss of 27.05% (calculated 28.28%) attributed to the loss of ($2CH_3N_2S$) moiety. Finally at above 750°C temperature the complex was completely decomposed and removed as Cd/CdO of 24.0% (calculated 21.19%). The different TG and DTG data are given in Table-9.

3.6.4. Antibacterial activity

The prime objective of performing the antibacterial screening is to determine the susceptibility of the pathogenic microorganism to test the compound which, in turn, is used to a selection of the compound as a therapeutic agent. The free Schiff base ligand and their metal complexes were screened for their antibacterial activity against strains the *Bacillus cereus ATCC25923*, *Streptococcus agelactiae*, *Escherichia coli ATCC 25922*, *Shigella dysenteriae* The compounds were tested at a concentration of 30 µg/0.01 mL in DMSO solution using the paper disc diffusion method with Kanamycin as standard. The susceptibility zones were measured in diameter (mm) and the result are listed in Table-10. The susceptibility zones were the clear zones around the discs killing the bacteria.

Table 10. Antibacterial activities of the complexes.

Bacterials strains	Zone of inhibition, diameter in mm						
	A (10µg /disc)	B (10µg /disc)	C (10µg /disc)	D (10µg /disc)	E (10µg /disc)	F (10µg /disc)	K (30µg /disc)
Gram positive							
Bacillus cereus	22	10	19	12	11	14	36
Streptococcus agelactiae	19	09	21	08	14	16	35

Gram negative							
Escherichia coli	23	12	24	09	12	18	32
Shigella dysenteriae	09	11	10	12	08	14	36

Where, A = $[C_{16}H_{16}ZnO_2N_6S_2].2H_2O$, B = $[C_{16}H_{16}NiO_2N_6S_2].H_2O$, C = $[C_{16}H_{16}MnO_2N_6S_2].H_2O$, D = $[C_{16}H_{16}SnO_2N_6S_2]$, E = $[C_{28}H_{18}CoO_6N_2].2H_2O$, F = $[C_{18}H_{22}CdO_2N_6S_2]$ and K = Kanamycin

4. Conclusions

In this paper we have explored the synthesis and coordination Chemistry of Ni(II), Zn(II), Mn(II), Sn(II), Co(II) and Cd(II) ions were synthesized with three different synthesized Schiff base ligands viz (L^1) [2-(2-hydroxybenzylidene)hydrazinecarbothioamide, (L^2) [4-((4-hydroxybenzylidene)amino)benzoic acid and (L^3) [2-(4-methoxybenzylidene)hydrazinecarbothioamide]. The ligands and metal complexes were characterized by molar conductivity measurement, magnetic susceptibility, Infrared, electronic spectral, thermal analysis and some physical measurements. The overall reactions were monitored by TLC analysis. Molar conductance study has shown that all the complexes were non-electrolytic in nature. FTIR studies suggested that Schiff bases act as deprotonated bidentate ligands and metal ions are attached with the ligands-(L^1), (L^2) by N, O and ligand-(L^3) by N, S coordinating sites during complexation reaction. Magnetic susceptibility data coupled with electronic spectra revealed that $[ZnC_{16}H_{16}O_2N_6S_2].2H_2O$, $[MnC_{16}H_{16}O_2N_6S_2].H_2O$, $[SnC_{16}H_{16}O_2N_6S_2]$ and $[CdC_{18}H_{22}O_2N_6S_2]$ complexes have tetrahedral, $[NiC_{16}H_{16}O_2N_6S_2].H_2O$ has a square planer and $[CoC_{28}H_{18}O_6N_2].2H_2O$ has octahedral geometry. Thermal analysis (TGA and DTG) data showed the possible degradation pathway of the complexes and also indicated that most of the complexes were thermally stable up to 200^0C. The Schiff bases and their metal complexes have been found moderate to strong antimicrobial activity.

REFERENCES

[1]. Angela Kriza, Lucica Viorica Ababei, Nicoleta Cioatera, Ileana Rău And Nicolae Stănică, Synthesis And Structural Studies Of Complexes Of Cu, Co, Ni And Zn With Isonicotinic Acid Hydrazide And Isonicotinic Acid (1-Naphthylmethylene)Hydrazide, J. Serb. Chem. Soc., 2010;75 (2):229- 242.

[2]. P. K. Das, N. Panda, N. K. Behera, Synthesis, Characterization and Antimicrobial Activities of Schiff Base Complexes Derived from Isoniazid and Diacetylmonoxime, IJISET – Int. J. of Innovative Sci., Eng. & Tech., 2016;3(1): 42-54.

[3]. Anil Kumar M R, Shanmukhappa S, Rangaswamy B E, Revanasiddappa M, Synthesis, Characterization, Antimicrobial Activity, Antifungal Activity and DNA Cleavage Studies of Transition Metal Complexes with Schiff Base Ligand, Int. J. of Innovative Sci., Eng. & Tech., 2015;4(2): 60-66.

[4]. O' Boyle N M, Tenderholt A L & Langer K M, cclib: a library for package-independent computational chemistry algorithms J. Comput. Chem., 2008; 29:839.

[5]. Saud I. Al-Resayes, Mohammad Shakir, Ambreen Abbasi, Kr. Mohammad Yusuf Amin, Abdul Lateef, Synthesis, spectroscopic characterization and biological activities of N4O2 Schiff base ligand and its metal complexes of Co(II), Ni(II), Cu(II) and Zn(II), Spectromica Acta Part A , 2012; 93:86-94.

[6]. K.D. Karlin, Z. Tyeklar, Bioinorganic Chemistry of Copper, Chapman & Hall: New York, 1993;101-109.

[7]. V. Arun, N. Sridevi, P.P. Robinson, S. Manju, K.K.M. Yusuff, "Ni(II) and Ru(II) Schiff base complexes as catalysts for the reduction of benzene" J. Mol. Catal. A: Chem., 2009; 304 (1-2):191-198.

[8]. K. C. Gupta, A. K. Sutar, Catalytic activities of Schiff base transition metal complexes, Coord. Chem. Rev., 2008; 252 (12-14):1420-1450.

[9]. R. I. Kureshy, N. H. Khan, S. H. R. Abdi, P. Iyer and S. T. Patel ,Chiral Ru(II) Schiff base complexes catalysed enantio selective eposidation of styrene derivatives using iodosyl benzene as oxidant II, J. Mol. Catal., 1999;150(1-2):175-183.

[10]. Saud I. Al-Resayes, Mohammad Shakirb, Ambreen Abbasi, Kr. Mohammad Yusuf Amin, Abdul Lateef, Spectromica Act.a Part A, 2012;93:86-94.
[11]. Rakesh Ranjan and Dhanashree S Hallooman, Synthesis And Characterization Of Co(Ii) And Ni(Ii) Complexes With Schiff Base 2,2-Dimethylpropiophenonethiosemicarbazone, Int. J. of Res. In Pharm. And Chem., 2014;4(2):423-426.
[12]. Angela Kriza, Mariana Loredana Dianu, Nicolae Stănicã, Constantin Drăghici, Mona Popoiu, Synthesis and Characterization of Some Transition Metals Complexes with Glyoxalbis-Isonicotinoyl Hydrazone, 2009;60(6):555-560.
[13]. L. Mitu, A. Kriza, Synthesis and Characterization of Complexes of Mn(II), Co(II), Ni(II) and Cu(II) with an Aroylhydrazone Ligand. Asian J. Chem., 2007;19 (1):658-664.
[14]. Ljubijankić N., Tešević V., Grgurić-Šipka S., Jadranin M., Begić S., Buljubašić L., Markotić E., Ljubijankić S., Synthesis and characterization of Ru(III) complexes with thiosemicarbazide-based ligands, 2016;47:1-6.
[15]. Methak. S. Mohammad, Preparation and Characterization of Some Transition Metal Complexes withSchiff base of thiosemicarbazone, J. of Kerbala Uni., Scien. 2010;8 (1):8-17 .
[16]. R.V. Singh, N. Fahmi and M.K. Biyala, Coordination Behavior and Biopotency of N and S/O Donor Ligands with their Palladium(II) and Platinum(II) Complexes, J. of the Ir. Chem. Soc., 2005;2(1):40-46.
[17]. A. M. Vijey, G. Shiny, and V. Vaidhyalingam, Synthesis and antimicrobial activities of 1-(5-substituted-2-oxo indolin-3-ylidene)-4-(substituted pyridin-2-yl) thiosemicarbazide, Arkivoc (xi)., 2008;187.
[18]. Mohammad Asif, A Review On Biological Activities Of Benzimidazole, Oxadiazole And Mannich Base Derivatives Of Benzimidazole-Oxadiazole Merged Compounds, Int. J. of Cur. Res. in App. Chem. & Chem. Eng., 2017;3(1):20-29.
[19]. M. M. H. Khalil, M. M. Abdaly and R. M. Ramadan, Spectroscopic and electrochemical studies of ruthenium and osmium complexes of salicylideneimine-2-thiophenol Schiff base, Spectrochimica Acta Part A: Mol. and Bio. Spec.., 2005;61(1):157-161.
[20]. P. M. Dahikar, R. M. Kedar, Synthesis, spectral and biological activity of transition metal complexes of substituted benzoinsemicarbazones, Inter. J. of Appl. or Inn. in Engg. & Man. (IJAIEM), 2013;2(4):8-11.
[21]. P. Murali Krishna, B. S. Shankara, and N. Shashidhar Reddy, Synthesis, Characterization, and Biological Studies of Binuclear Copper(II) Complexes of (2E)-2-(2-Hydroxy-3-Methoxybenzylidene)-4N-Substituted Hydrazine carbothioamides, Hindawi Publishing Corporation, International Journal of Inorganic Chemistry, 2013,11pages.
[22]. Ljiljana S. Vojinović-Ješić, Vukadin M. Leovac, Mirjana M. Lalović, Valerija I. Češljević, Ljiljana S. Jovanović, Marko V. Rodić and Vladimir Divjaković, Transition metal complexes with thiosemicarbazide-based ligands. Part 58. Synthesis, spectral and structural characterization of dioxovanadium(V) complexes with salicylaldehydethiosemicarbazone, J. Serb. Chem. Soc. 2011;76 (6):865–877.
[23]. Monika Tyagi, Sulekh Chandra, Synthesis, characterization and biocidal properties of platinum metal complexes derived from 2,6-diacetylpyridine (bisthiosemicarbazone), Open Jo. of Inorg. Chem., 2012;2:41-48.
[24]. Vojinović-JešićLJ. S., LeovacV.M., LalovićM. M., ČešljevićV.I., Jovanović Lj.S.Rodić M. V. and Divjaković V, Transition metal complexes with thiosemicarbazide-based ligands. Part 58. Synthesis, spectral and structural characterization of dioxovanadium(V) complexes with salicyl aldehyde thiosemicarbazone, J. Serb. Chem. Soc., 2011;76 (6):865–877.
[25]. Baiu S.H., El-Ajaily M.M. and El-Barasi, Antibacterial Activity of Schiff Base Chelates of Divalent Metal Ions, Asian Journal of Chemistry, (2009);21(1):5-10.
[26]. Elena Pahontu, ValeriuFala , Aurelian Gulea , Donald Poirier, Victor Tapcov and Tudor Rosu, Synthesis and Characterization of Some New Cu(II), Ni(II) and Zn(II) Complexes with Salicylidene Thiosemicarbazones: Antibacterial, Antifungal andin Vitro Antileukemia Activity, Molecules, 2013;18:8812-8836.
[27]. El-Bahnasawy R. M., Sharaf El-Deen L.M., El-Table A.S., Wahba M. A. and El-Monsef. A., Electrical Conductivity Of Salicylaldehyde Thiosemicarbazone and its Pd(II), Cu(II) and Ru(III) Complexes, Eur. Chem. Bull, 2014;3(5):441-446.
[28]. Md. Saddam Hossain, C.M. Zakaria, M.M.Haque, and Md. Kudrat-E-Zahan, Spectral and thermal characterization with antimicrobial activity on Cr(III) and Sn(II) Complexes containing N,O Donor novel schiff base ligand, Int. J. of Chem. Studies., 2016;4(6):08-11.

[29]. A. Xavier, P. Gopu ,B. Akila,K. Suganya, Synthesis and Characterization of Schiff Base from 3, 5-Di ChloroSalicylaldehyde with 4-Bromoaniline and 4-Aminobenzoic Acid and Its 1st Row Transition Metal Complexes, Int. J. of Inn. Res. & Dev., 2015;4(8):384-396 .
[30]. Manohar V. Lokhande and Mrityunjay R. Choudhary, Some Transitional Metal Ions Complexes With 3-{[(E)-(4-Fluorophenyl) Methylidene] Amino} Benzoic Acid And Its Microbial Activity, International Journal of Pharmaceutical Sciences and Research, IJPSR, 2014;5(5):1757-1766.
[31]. P. Gopu, Dr. A. Xavier, Synthesis and Characterization of 4-(3-bromo-5 -chloro-2-hydroxybenzlidimino) Benzoic Acid and its Transition Metal Complexes, International Journal of Science and Research (IJSR), 2015;4(8):15-21.
[32]. Shanker K, Rohini R, Ravinder V and Reddy P M: Ru(II) complexes of N_4 and N_2O_2 macrocyclic Schiff base ligands: Their antibacterial and antifungal studies, Spectro chimica Acta A, 2009;73:l205-211.
[33]. Raju Ashokan, Saravanan Sathishkumar, Ekamparam Akila And Rangappan Rajavel, Synthesis, Characterization and Biological Activity of Schiff Base Metal Complexes Derived from 2, 4-Dihydroxyactophenone, Chemical Science Transactions , 2017; 6(2):277-287 .
[34]. Miguel-Angel Munoz-Hernandes, Michal L. Mckee, Timothy S. Keizer, Burt C. Yearwood and David Atwood, Six-coordinate aluminiumcations: characterization, catalysis, and theory, 2002;3.
[35]. K. Nakamoto: Infrared Spectra of Inorganic and Coordination Compounds. John Wiley & Sons, New York, 2nd Edition, 1970.
[36]. Shanker K B, Rohini M, Ravinder Reddy P and Ho M Y P: Synthesis of Tetraaza Macrocyclic Pd(II) complexes; Antibacterial & Catalytic studies, J.of the Ind. Chem. Soc. 2009, 86.
[37]. K.P. Satheesh, V. Suryanarayana Rao, Spectrophotometric Method For The Determination Of Trace Amount Of Tungsten (Vi) In Alloy Samples Using 4-Hydroxybenzaldehydethiosemicarbazon, J. of Adv. Scien. Res., 2015; 6(2): 14-17.
[38]. S. Janarthanan, Y.C. Rajan, P.R. Umarani, D. Jayaraman, D. Premanand and S. Pandi, Synthesis, growth, optical and thermal properties of a new organic crystal semicarbazone of p-anisaldehyde, (SPAS), 2010;3(8):42-47.
[39]. Ruchi Agarwal, Mohd. Asif Khan and Shamim Ahmad, Schiff base complexes derived from thiosemicarbazone, synthesis characterization and their biological activity , Journal of Chemical and Pharmaceutical Research, 2013;5(10):240-245.
[40]. Sandra S. Konstantinovi, Blaga C. Radovanovi, IvojinCaki And VesnaVasi, Synthesis and characterization of Co(II), Ni(II), Cu(II) and Zn(II) complexes with 3-salicylidenehydrazono-2-indolinone,J.Serb.Chem.Soc., 2003;68(8–9):641–647.
[41]. N. K. Gondia, J. Priya, S. K. Sharma, Synthesis and physico-chemical characterization of a Schiff base and its zinc complex, Res Chem Intermed, 2017;43:1165–1178.
[42]. Lotf A. Saghatforoush, Ali Aminkhani, Sohrab Ershad, Ghasem Karimnezhad, Shahriar Ghammamy and Roya Kabiri, Preparation of Zinc (II) and Cadmium (II) Complexes of the Tetradentate Schiff Base Ligand 2-((E)-(2-(2(pyridine-2-yl)-ethylthio)ethylimino)methyl)-4-bromophenol (PytBrsalH), Molecules 2008;13:804-811.
[43]. Jian-Ning Liu, Bo-Wan Wu, Bing Zhang, Yongchun Liu, Synthesis and Characterization of Metal Complexes of Cu(II), Ni(II), Zn(II), Co(II), Mn(II) and Cd(II) with Tetradentate Schiff Bases, Turk J Chem., 2006;30:41-48.
[44]. Shayma A. Shaker, Preparation and Spectral Properties of Mixed-Ligand Complexes of VO(IV), Ni(II), Zn(II), Pd(II), Cd(II) and Pb(II) with Dimethylglyoxime and N-Acetylglycine, E-Journal of Chemistry, 2010;7(S1):S580-S586.
[45]. Md. Kudrat-E-Zahan, M. S. Islam, and Md. Abul Bashar ,Synthesis, Characteristics, and Antimicrobial Activity of Some Complexes of Mn(II), Fe(III) Co(II), Ni(II), Cu(II), and Sb(III) Containing Bidentate Schiff Base of SMDTC, Russian Journal of General Chemistry, 2015;85(3):667–672.
[46]. Rehab K. Al-Shemary, Ahmed T. Numanand Eman Mutar Atiyah, Synthesis, Characterization And Antimicrobial Evaluation Of Mixed Ligand Complexes Of Manganese(Ii), Cobalt(Ii), Copper(Ii), Nickel(Ii) And Mercury(Ii) With 1,10-Phenanthroline And A Bidentate Schiff Base, Eur. Chem. Bull., 2016;5(8):335-338.
[47]. Iniama, G.E., Olarele, O.S. and Johnson, A, Synthesis, spectral, characterization and antimicrobial activity of manganese (II) and copper (II) complexes of Salicylaldehydephenylhydrazone, Int. J. of Chem. and Appl., 2015;7(1):15-23.
[48]. Neelofar, Nauman Ali, Shabir Ahmad, Naser M. Abdel-Salam, Riaz Ullah, Robila Nawaz and Sohail Ahmad, Synthesis and evaluation of antioxidant and antimicrobial activities of Schiff

base tin (II) complexes, Tropical Journal of l Pharmaceutical Research ,2016;15(12):2693-2700.
[49]. Har Lal Singh and J. B. Singh, Synthesis and Characterization of New Lead(II)and Organotin(IV) Complexes of Schiff Bases Derived from Histidine and Methionine, Hindawi Publishing Corporation, International Journal of Inorganic Chemistry, 2012,7pages.
[50]. Sunita Bhanuka and Har Lal Singh, Spectral, Dft And Antibacterial Studies Of Tin(Ii) Complexes Of Schiff Bases Derived From Aromatic Aldehyde And Amino Acids, Rasayan J. Chem., 2017; 10(2):673-68.
[51]. Khalil Abid, Sinann Al–Bayati, Anaam Rasheed, Synthesis, Characterization, Thermal study and Biological Evaluation of Transition Metal Complexes Supported by ONNNO-Pentadentate Schiff Base Ligand, American Journal of Chemistry, 2016;6(1):1-7.
[52]. Allan J. R. and Veitch P. M., The preparation, characterization and thermal analysis studies on complexes of cobalt(II) with 2-, 3-, 4-cyanopyridines, J. Thermal Anal., 1983; 27(1): 3-15.
[53]. Moamen S. Refat, I. M. El-Deen, M. S. El-Garib, and W. Abd El-Fattah, Spectroscopic and Anticancer Studies on New Synthesized Copper(II) and Manganese(II) Complexes with 1,2,4-Triazines Thiosemicarbazide1, Russian J. of Gen. Chem., 2015;85(3): 692–707.
[54]. Md. Saddam Hossain, Md. Ashraful Islam, C. M. Zakaria, M. M. Haque, Md. Abdul Mannan, Md. Kudrat-E-Zahan, Synthesis, Spectral and Thermal Characterization with Antimicrobial Studies on Mn(II), Fe(II), Co(II) and Sn(II) Complexes of Tridentate N,O Coordinating Novel Schiff Base Ligand" J. Chem. Bio. Phy. Sci. Sec. A., 2016;6 (1):041-052.
[55]. M. R. Islam, J. A. Shampa, M. Kudrat-E-Zahan, M. M. Haque, Y. Reza, Investigation on Spectroscopic, Thermal and Antimicrobial Activity of Newly Synthesized Binuclear Cr(III) Metal Ion Complex , J. Sci. Res., 2016;8 (2):181-189.
[56]. Sayed M. Abdallah, M.A. Zayed, Gehad G. Mohamed, Synthesis and spectroscopic characterization of new tetradentate Schiff base and its coordination compounds of NOON donor atoms and their antibacterial and antifungal activity, Arabian J. of Chem., 2010; 3:103–113.
[57]. Samir Alghool. Mononuclear complexes based on reduced Schiff base derived fromL-methionine, synthesis, characterization, thermal and in vitro antimicrobial studies, J Therm Anal Calorim, 2015; 12: 1309–1319.
[58]. Achut S. Munde, Amarnath N. Jagdale, Sarika M. Jadhav And Trimbak K. Chondhekar, Synthesis, characterization and thermal study of some transition metal complexes of an asymmetrical tetradentate Schiff base ligand, J. Serb. Chem. Soc., 2010;75(3):349–359.
[59]. A.S. Munde, V. A. Shelke, S. M. Jadhav, A. S. Kirdant, S. R. Vaidya, S. G. Shankarwar, and T. K. Chondhekar, Synthesis, Characterization and Antimicrobial Activities of some Transition Metal Complexes of Biologically Active Asymmetrical Tetradentate Ligands, Adv. Appl. Sci. Res., 2012; 3(1):175-182.

Supplementary Materials

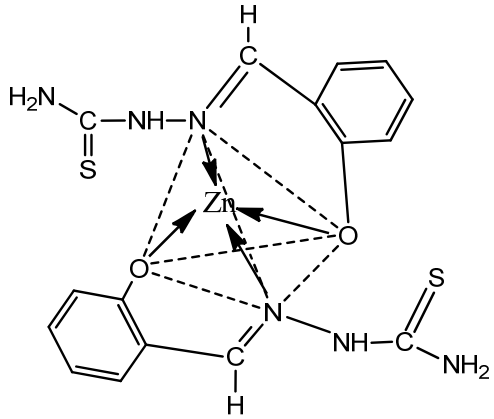

Figure: Structure of $[C_{16}H_{16}ZnO_2N_6S_2]$

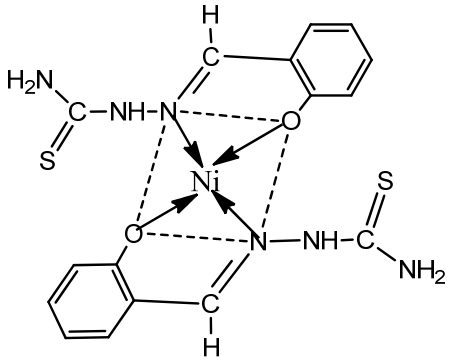

Figure: Structure of $[C_{16}H_{16}NiO_2N_6S_2]$

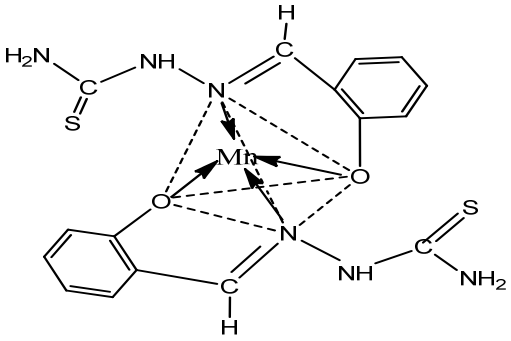

Figure: Structure of $[C_{16}H_{16}MnO_2N_6S_2]$

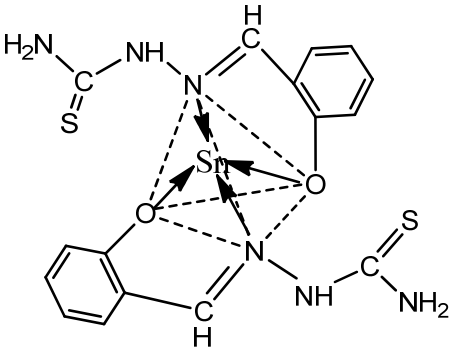

Figure: Structure of $[C_{16}H_{16}SnO_2N_6S_2]$

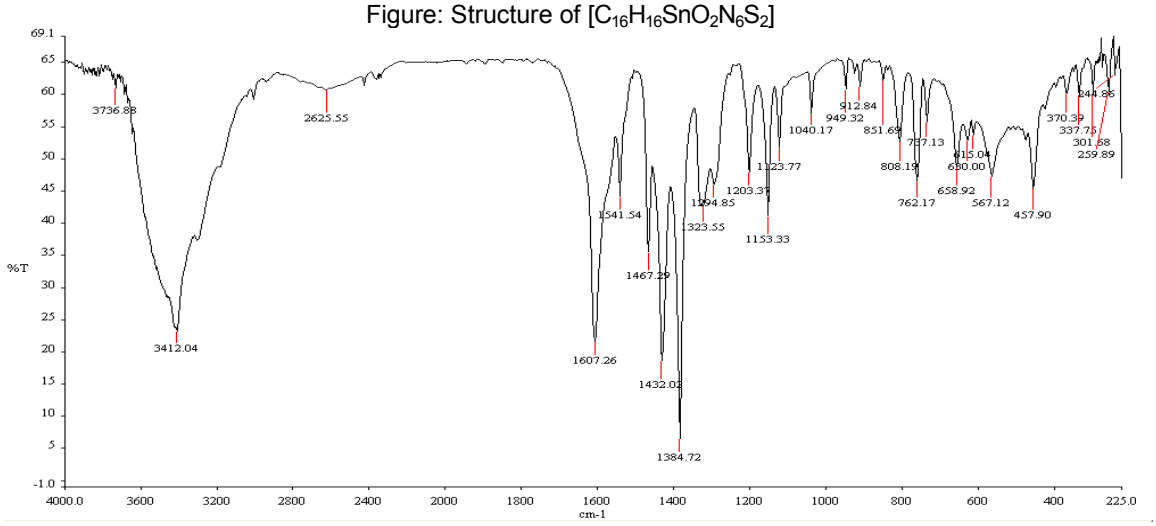

Figure: IR spectra of $[NiC_{16}H_{16}O_2N_6S_2].H_2O$

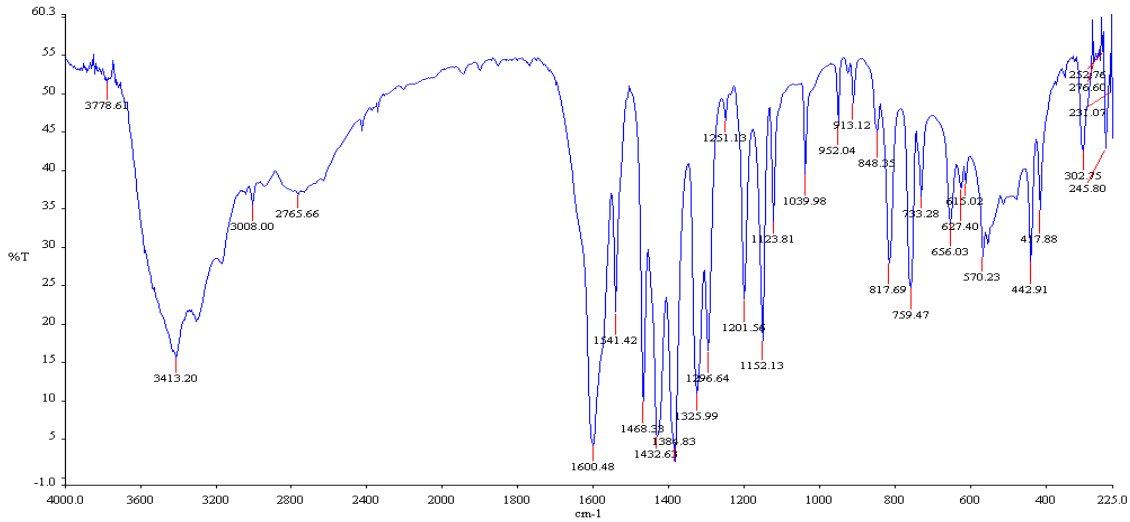

Figure: IR spectra of $[MnC_{16}H_{16}O_2N_6S_2].H_2O$

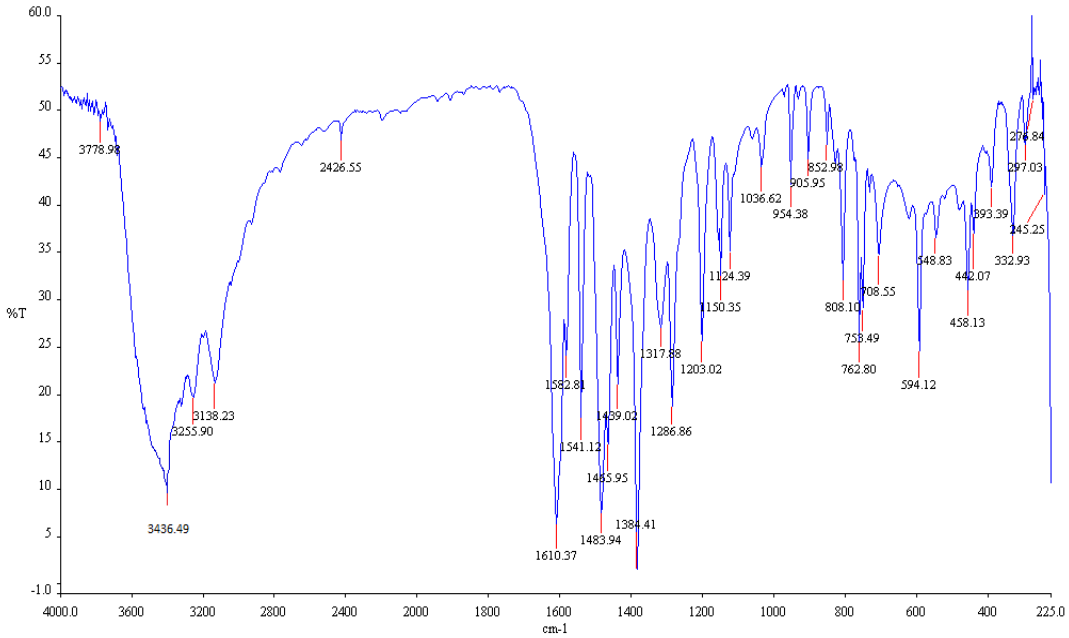

Figure: IR spectra of $[SnC_{16}H_{16}O_2N_6S_2]$

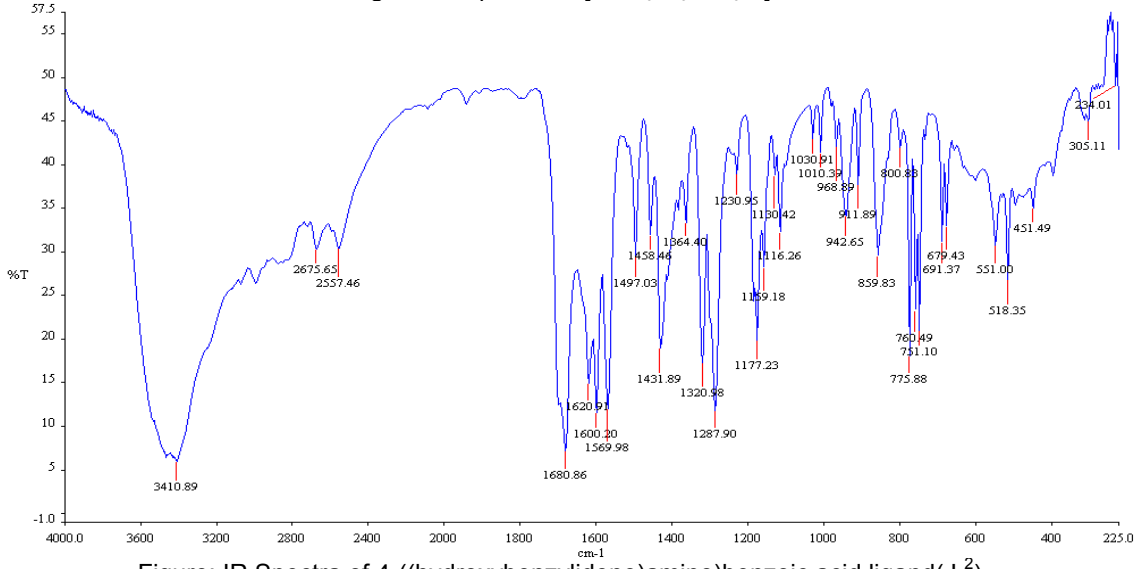

Figure: IR Spectra of 4-((hydroxybenzylidene)amino)benzoic acid ligand(L^2)

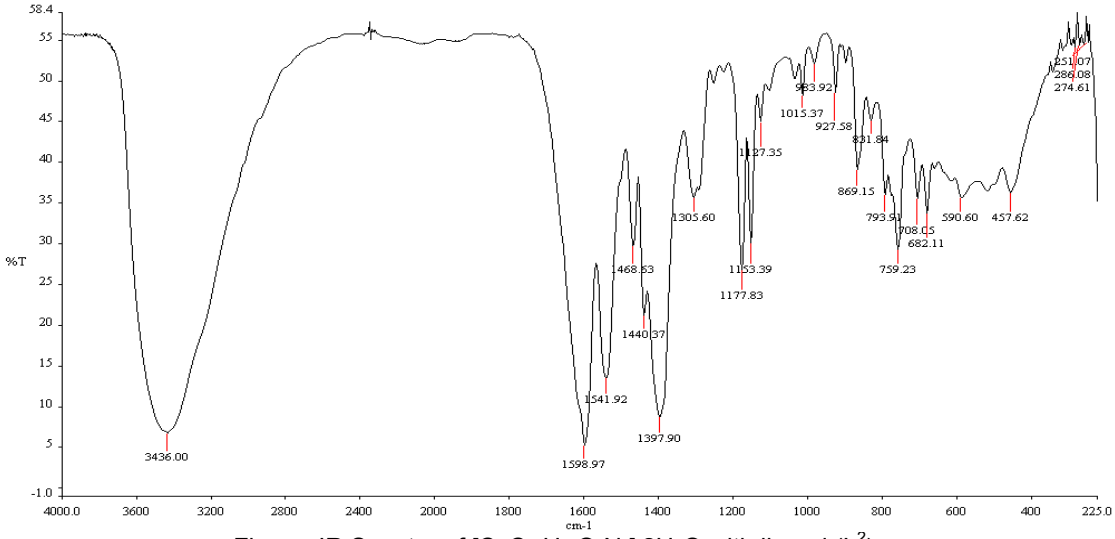

Figure: IR Spectra of $[CoC_{28}H_{18}O_6N_2].2H_2O$ with ligand (L^2)

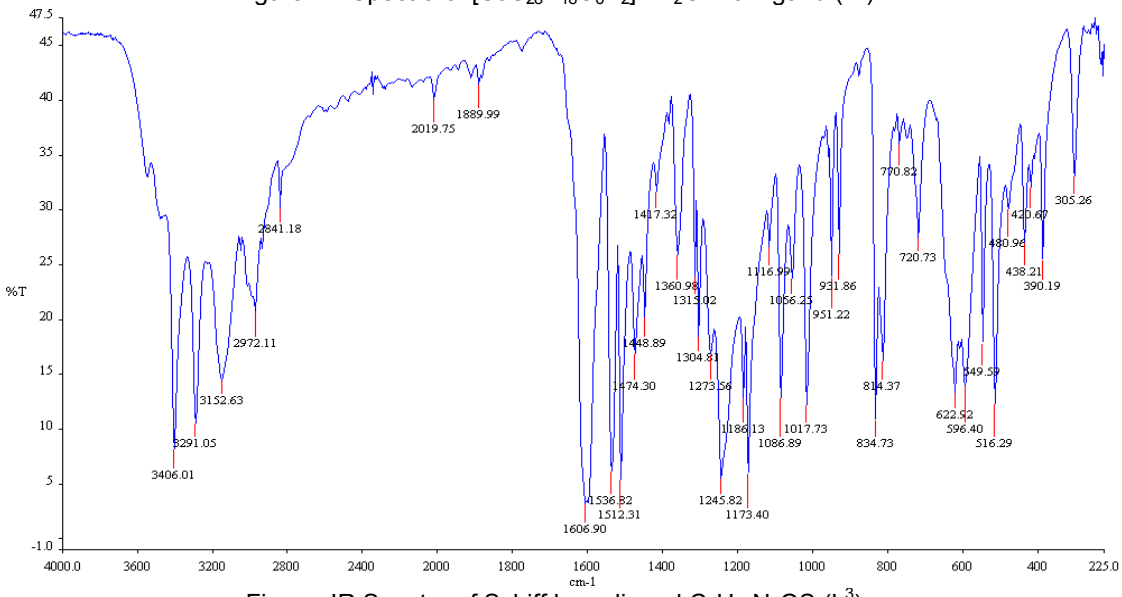

Figure: IR Spectra of Schiff base ligand $C_9H_{11}N_3OS$ (L^3)

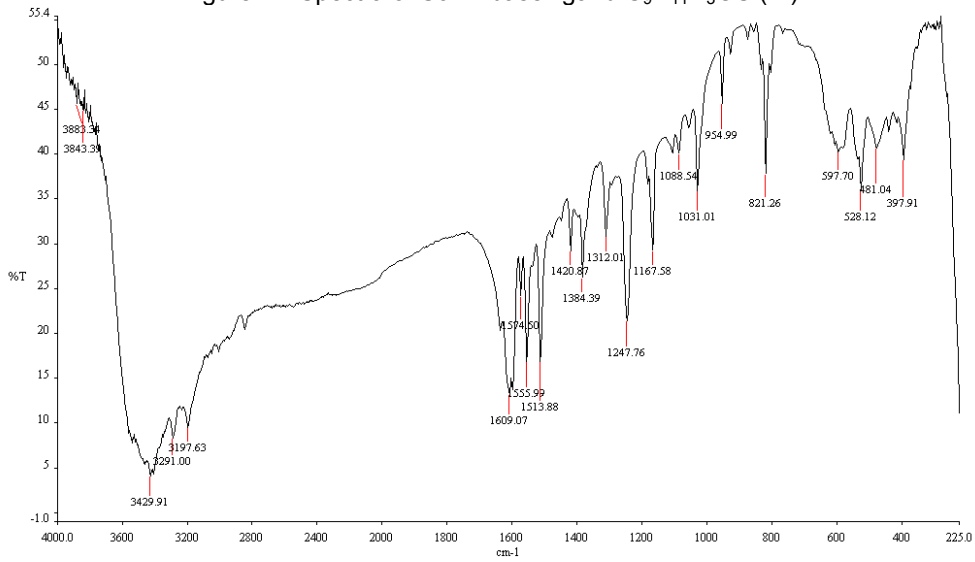

683 Figure: IR Spectra of $[CdC_{18}H_{22}O_2N_6S_2]$
684

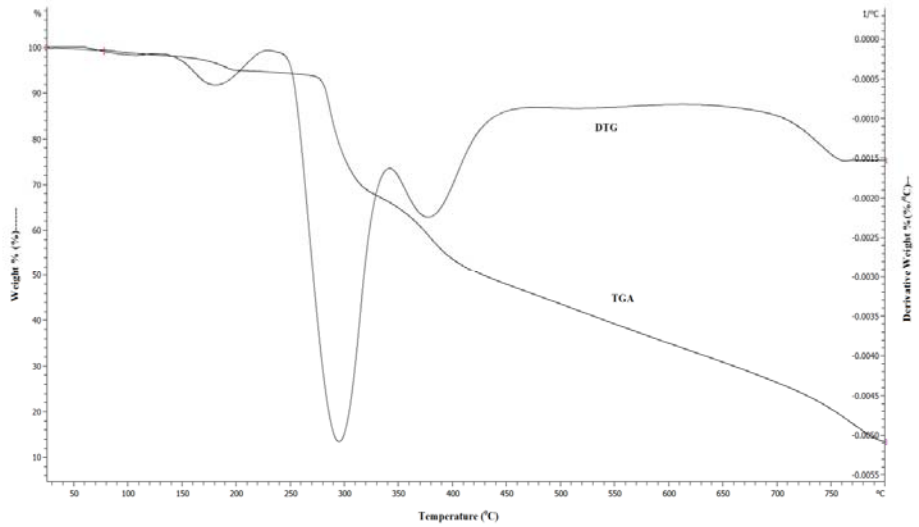

685
686 Figure: TGA and DTG curve of $[NiC_{16}H_{16}O_2N_6S_2].H_2O$

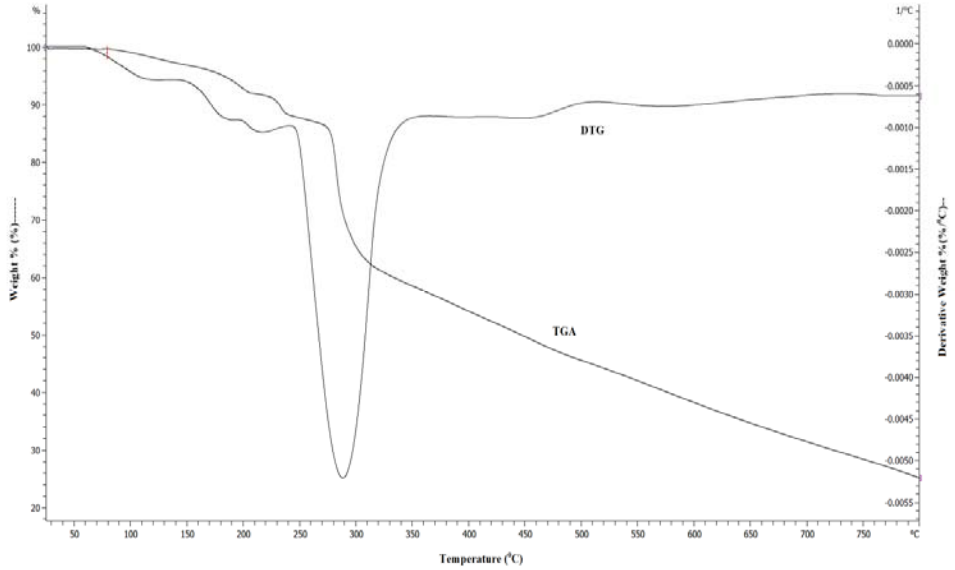

687
688 Figure: TGA and DTG curve of $[MnC_{16}H_{16}O_2N_6S_2].H_2O$
689

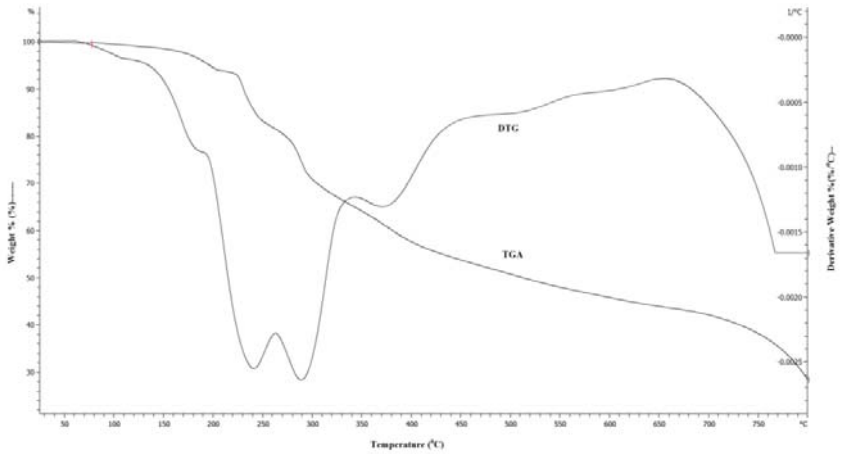

690
691 Figure: TGA and DTG curve of $[SnC_{16}H_{16}O_2N_6S_2]$
692

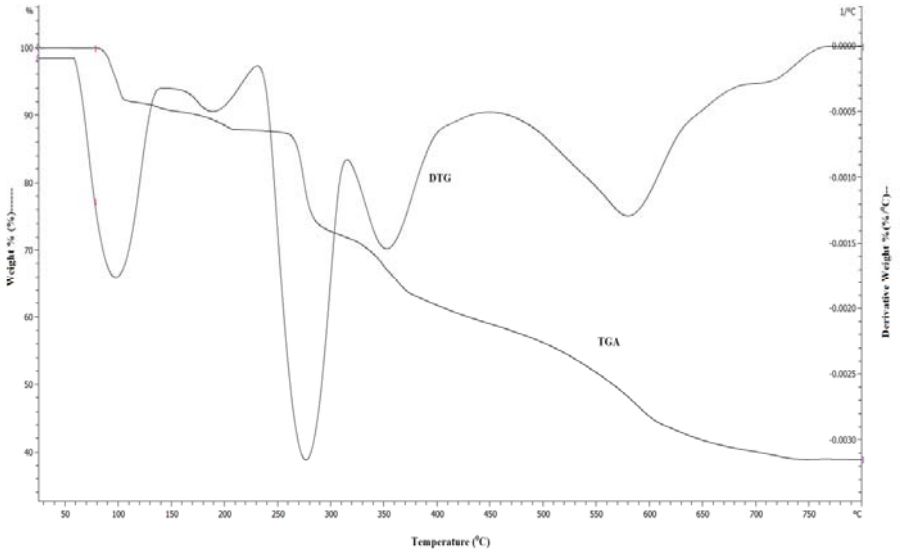

693
694 Figure: TGA and DTG curve of $[ZnC_{16}H_{16}O_2N_6S_2].2H_2O$

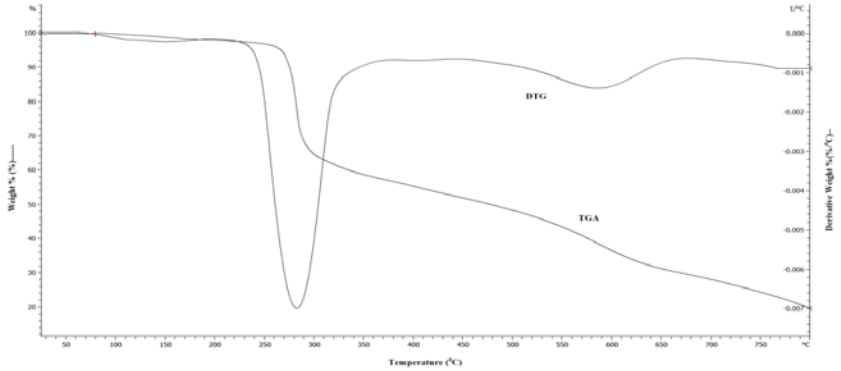

695
696 Figure: TGA and DTG curve of $[CdC_{18}H_{22}O_2N_6S_2]$
697